JSHC
Japan Society of
Histochemistry and Cytochemistry
Established 1959

Acta Histochem. Cytochem. 50 (3): 111–118, 2017
doi: 10.1267/ahc.17004

Expression of c-kit and Cytokeratin 5 in the Submandibular Gland after Release of Long-Term Ligation of the Main Excretory Duct in Mice

Hiroshi Watanabe[1], Haruka Takahashi[2], Miyuki Hata-Kawakami[2] and Akira Tanaka[2]

[1]Course of Clinical Science, Field of Oral and Maxillofacial Surgery and Systemic Medicine, Oral and Maxillofacial Surgery, The Nippon Dental University Graduate School of Life Dentistry at Niigata, 1–8 Hamaura-cho, Chuo-ku, Niigata, Japan and [2]Department of Oral and Maxillofacial Surgery, School of Life Dentistry, The Nippon Dental University at Niigata, Japan

Received January 18, 2017; accepted May 31, 2017; published online June 22, 2017

Long-term submandibular duct obstruction is thought to cause irreversible atrophy and dysfunction of the submandibular gland. As an atrophic gland may be induced clinically by chronic or recurrent infection, it is generally removed surgically. However, the regenerative capacity of atrophic submandibular glands after long-term obstruction is not completely understood. We studied the regenerative capacity of the mouse submandibular duct using an aneurysm clip ligation model. We documented changes in the size, histologic structure and gene expression of the submandibular gland after 2 months of ligation, and 1 week, 1 month and 2 months after clip removal. Two months of ligation caused atrophy, particularly in the acinar portion. In the 2 months after clip removal, we observed a steady and significant increase in the expression of the acinar cell precursor gene cytokeratin 5 (CK5), and a significant decrease in the expression of the stem cell marker c-kit. These findings suggest that the submandibular gland retains some capacity for regeneration even after long-term obstruction, and that CK5 could serve as a marker of this regenerative process.

Key words: salivary gland, duct ligation, regeneration, c-kit, cytokeratin 5 (CK5)

I. Introduction

It is well recognized that the atrophy provoked by obstruction of the salivary ducts induces changes in the structure [1, 2, 31, 32, 35], the residual function and the regenerative capacity of the glandular tissue [4, 9, 19, 28]. Almost all the evidence is based on short-term experiments conducted over approximately 1 week, and there have been no longer-term observational studies. The structural changes and the functional improvements in atrophied salivary glands after release from long-term obstruction, for example by salivary calculi, is still not known. To date, the longest period of experimental obstruction of the main salivary gland duct has been 3 months, in a study that identified the expression of a stem cell marker in atrophied salivary glands [17]. The regenerative capacity of salivary glands after the release of long-term obstruction has not yet been examined.

In this study, we examined the temporal changes that occurred in glandular tissue after release of long-term salivary gland obstruction *in vivo*. For this purpose we created a model of obstruction of the main excretory duct of the submandibular gland, using an aneurysm clip in mice. After releasing the ligation, we examined the time-dependent changes in tissue structure, residual function and regenerative capacity in the atrophied salivary glands.

Correspondence to: Hiroshi Watanabe, Course of Clinical Science, Field of Oral and Maxillofacial Surgery and Systemic Medicine, Oral and Maxillofacial Surgery, The Nippon Dental University Graduate School of Life Dentistry at Niigata, 1–8 Hamaura-cho, Chuo-ku, Niigata 951–1500, Japan. E-mail: watahiro@ngt.ndu.ac.jp

II. Materials and Methods

Animals

Experimental animals were 10-week-old female ICR mice (CLEA Japan, Tokyo, Japan), housed in a 12-hr light-dark cycle and given free access to solid food (Oriental

Yeast, Tokyo, Japan) and water. Conduct of the study was approved by the Animal Experiment Ethics Committee of the Nippon Dental University School of Life Dentistry in Niigata (approval reference number 170).

Ligation of the main excretory duct of the submandibular salivary gland and tissue collection

Twenty mice were anesthetized by intraperitoneal administration of pentobarbital sodium 30 mg/kg and xylazine hydrochloride 10 mg/kg and fixed in the dorsal position. Using a stereomicroscope, the submandibular gland was exposed by blunt dissection of the skin in the midline of the neck to prevent damage to the surrounding nerves, vessels and other tissues. The main excretory duct was clipped approximately 2 mm superior to the main body of the right submandibular gland with a Sugita titanium aneurysm clip (Mizuho Ika Kogyo, Tokyo, Japan), following which the wound was closed. The left submandibular gland was not clipped and served as a control. The same approach was used to remove the clip 2 months later. The duration of ligation was informed by a previous study that reported no significant difference in the expression of c-kit, Sca-1, or cytokeratin 5 (CK5), which were judged to participate in salivary gland regeneration, after 2 or 3 months of obstruction [17]. Submandibular gland tissue samples were collected after 2 months of ligation, and then 1 week, 1 month or 2 months after the release of ligation. Experimental animals were therefore divided into the following groups, with five animals per group: 2-month ligation (2M lig group); 2-month ligation and 1 week after de-ligation (2M+1W del group); 2-month ligation and 1 month after de-ligation (2M+1M del group); and 2-month ligation and 2 months after de-ligation (2M+2M del group). For final tissue collection, animals were terminally anesthetized and perfused with phosphate-buffered saline (9.57 mM, pH 7.35–7.65, Takara Bio, Shiga, Japan) then fixed with 4% paraformaldehyde (PFA, Wako Pure Chemical Industries, Osaka, Japan) via a thoracotomy.

Submandibular gland measurement

The dimensions of the major and minor axes of the submandibular glands were measured with calipers before collecting tissue for analysis of gene expression. Paired two-way analysis of variance (ANOVA) and Bonferroni multiple comparisons were performed for statistical analysis (Ekuseru-Toukei 2015: Social Survey Research Information, Tokyo, Japan). A p value < 0.05 was considered statistically significant.

Tissue preparation and general staining

Samples for histologic analysis underwent immersion fixation with 4% PFA (Wako Pure Chemical Industries), were dehydrated in an ascending ethanol series and were embedded in paraffin. A rotating microtome was used to create 5-μm slices, which were subject to hematoxylin-eosin (HE) staining. Histologic observations were performed with an optical microscope (Olympus BX51, Tokyo, Japan).

Table 1. *List of primary antibodies*

Antibody	Provider (catalog number)	Dilution
Anti-c-kit	Abcam (ab5506)	1:1,000
Anti-cytokeratin 5	Covance (PRB-160P)	1:3,000
Anti-aquaporin 5	Abcam (ab104751)	1:2,000
Anti-α-amylase	Sigma-Aldrich (A8273)	1:1,000

Providers: Abcam (Tokyo, Japan), Covance (Princeton, NJ, US), Sigma-Aldrich (St. Louis, USA).

Immunohistochemistry

The immunohistochemical expression of c-kit, CK5, aquaporin 5 (AQP5) and α-amylase were assessed. Slices of paraffin-embedded tissue were deparaffinized and rehydrated in a xylene-ethanol series. Endogenous peroxidase blocking (Dako REAL™ peroxidase blocking solution, Agilent Technologies, Santa Clara, CA, USA) and antigen activation (HistoVT One, Nacalai Tesque, Kyoto, Japan) were performed on the treated slices. They were subsequently incubated with primary then secondary antibodies (EnVision™ + Dual link System-HRP, Agilent Technologies), and binding was reported with 3,3′-diaminobenzidine (ImmPACT™ DAB, Vector Laboratories, Burlingame, CA, USA). After the nuclei were stained with hematoxylin, specimens were cleared and mounted. Table 1 shows the primary antibodies used in this experiment.

RNA preparation and real-time reverse transcription polymerase chain reaction

After collection, tissue samples were immediately immersed in RNA*later* RNA stabilization reagent (Qiagen, Holden, Germany) and stored until use. Total RNA was extracted with ISOGEN II (Wako Pure Chemical Industries). After purification, complementary DNA (cDNA) was synthesized with a high-capacity cDNA reverse transcription kit (Life Technologies, Carlsbad, CA, USA). After cDNA synthesis, gene expressions of c-kit, CK5, AQP5, α-amylase and GAPDH were analyzed using the reverse transcription polymerase chain reaction (RT-PCR) and quantified with real-time PCR. A reaction solution was prepared with Fast SYBR® Green Master Mix (Applied Biosystems, Foster City, CA, USA) using appropriate primers (Table 2). Real-time RT-PCR was performed using StepOnePlus™ (Applied Biosystems). After initial heating at 95°C for 20 sec, PCR conditions were set at 95°C for 3 sec and 60°C for 30 sec for 40 cycles each. The levels of RNA expression in the 2M lig group were considered as baseline and were analyzed using the ΔΔCT method. Paired two-way ANOVA and Bonferroni multiple comparisons were performed for statistical analysis (Ekuseru-Toukei 2015). A p value < 0.05 was considered statistically significant.

Table 2. *Primer sequences*

Gene target	Sequence 5′-3′	GenBank accession number	Product size
c-kit	F: ACGCCAGGAGACGCTGACTA	NM_001122733.1	105
	R: AAGGTTGTTGTGACATTTGCTGAT		
Cytokeratin 5	F: TCCTCCAGGAACCATCATGTCT	NM_027011.2	125
	R: GGGACACCGAGCTGAAGCT		
Aquaporin 5	F: CCTTCTTCAAGGCCGTGTTC	NM_009701.4	120
	R: AGGCTATGGAGATCTGCAGAATG		
α-Amylase	F: CGAACTGCTATTGTCCACCTGTT	NM_001110505.1	120
	R: GATGTTTTCATTGGGTGGAGAGA		
GAPDH	F: AGGTTGTCTCCTGCGACTTCA	NM_001289726.1	100
	R: CAGGAAATGAGCTTGACAAAGTTG		

Abbreviations: F, forward; R, reverse; GAPDH, glyceraldehyde-3-phosphate dehydrogenase.

III. Results

Submandibular gland measurement

The major and minor axes of the submandibular gland were significantly smaller in the ligated side of all experimental groups (2M lig, 2M+1W del, 2M+1M del, and 2M +2M del groups) than the control side at all time points. There were no significant changes in the size of the glands after the release of ligation in the experimental groups.

Histologic analysis

The acinar portion was not atrophied in any of the glands taken from mice in the control group. In these animals, the acinar portion was round or elliptical with the cell nuclei displaced to the basal side, and intercalated ducts, granular ducts and striated ducts were easily distinguishable (Fig. 1A). However, signs of atrophied salivary gland tissue, such as atrophy and disappearance of the acinar portion, dilation of the ductal lumen, appearance of duct-like structures and proliferation of interlobular connective tissue, were observed in the 2M lig and 2M+1W del groups (Fig. 1B and 1C, respectively). In the 2M+1M del group, dilation of the ductal lumen, interlobular connective tissue and other signs of atrophied salivary gland tissue were evident, but were less prominent than those in the 2M lig group. In addition, a small acinar portion was observed in some areas (Fig. 1D). In the 2M+2M del group, there were fewer signs of atrophy of salivary gland tissue or the acinar portion; the latter was larger than those observed in the 2M +1M del group (Fig. 1E).

Immunohistochemistry analysis

In the control group, c-kit, which was used as a stem cell marker, and CK5, which was used as an acinar cell precursor marker, were observed in some ducts (Figs. 2A and 3A). As expected, AQP5, which had been selected as an acinar cell marker, was positive in the acinar portion [13]. α-Amylase, which was used to confirm functionality, was weakly positive in the acinar portion and strongly positive in the ducts. In the experimental groups, c-kit was positive in and around some ducts and duct-like structures in the 2M lig group (Fig. 2B). The number of c-kit positive cells was lower in the 2M+1W del group than in the 2M lig group, and were observed mainly around duct-like structures (Fig. 2C), but increasing numbers over time were identified in the 2M+1M del and 2M+2M del groups (Fig. 2D, E). There was positive CK5 staining in the ducts and some duct-like structures in the 2M lig group (Fig. 3B). In the post-release groups, localization of CK5 in duct-like structures tended to become more robust over time in the 2M+1W del, 2M +1M del and 2M+2M del groups (Fig. 3C–E). Notably, cells in many duct-like structures exhibited CK5-positive staining in the 2M+2M del group, although localization to the acinar portion was not observed (Fig. 3E). There was positive AQP5 staining in atrophied acinar portion-like cells in the 2M lig and 2M+1W del groups. In the 2M+1M del and 2M+2M del groups, there was AQP5 staining in the cellular membrane of the acinar portion. Almost no cells showed positive staining for α-amylase in any of the experimental groups (data not shown).

Gene expression analysis

Significant differences in gene expression were observed between controls and all experimental groups ($p < 0.01$, Fig. 4A–D). The c-kit expression level decreased significantly in the 2M+1W del group ($p < 0.01$), then increased significantly in the 2M+1W del and 2M+2M del groups ($p < 0.05$, Fig. 4A). The CK5 expression level increased significantly over time in all experimental groups ($p < 0.01$, Fig. 4B); however, AQP5 and α-amylase expression did not change significantly over time after deligation in any of the experimental groups (Fig. 4C, D).

IV. Discussion

The salivary glands are exocrine glands that secrete saliva into the oral cavity. Age, disease and other factors can block the ducts, causing salivary gland atrophy and functional decline. Obstructive salivary gland diseases seen in the clinic may be associated with long-term disease, such

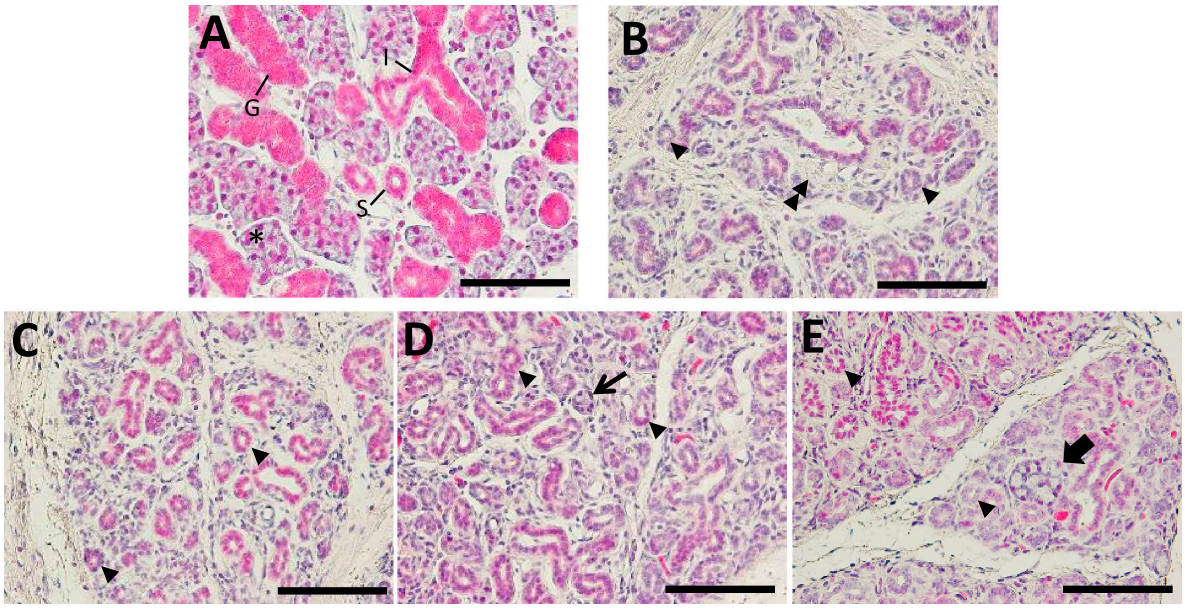

Fig. 1. Hematoxylin and eosin staining of the submandibular gland: **A**) controls; **B**) 2-month ligation (2M lig) group; **C**) 2-month ligation, 1 week after release (2M+1W del) group; **D**) 2-month ligation, 1 month after release (2M+1M del) group; **E**) 2-month ligation, 2 months after release (2M+2M del) group. Structures are identified as follows: asterisk, acinar portion; I, intercalated ducts; G, granular duct; S, striated duct; open arrow, small acinar portion after de-ligation; double arrowhead, proliferation of interlobular connective tissue; arrow, acinar portion after de-ligation; arrowhead, duct-like structure. Bar = 100 μm.

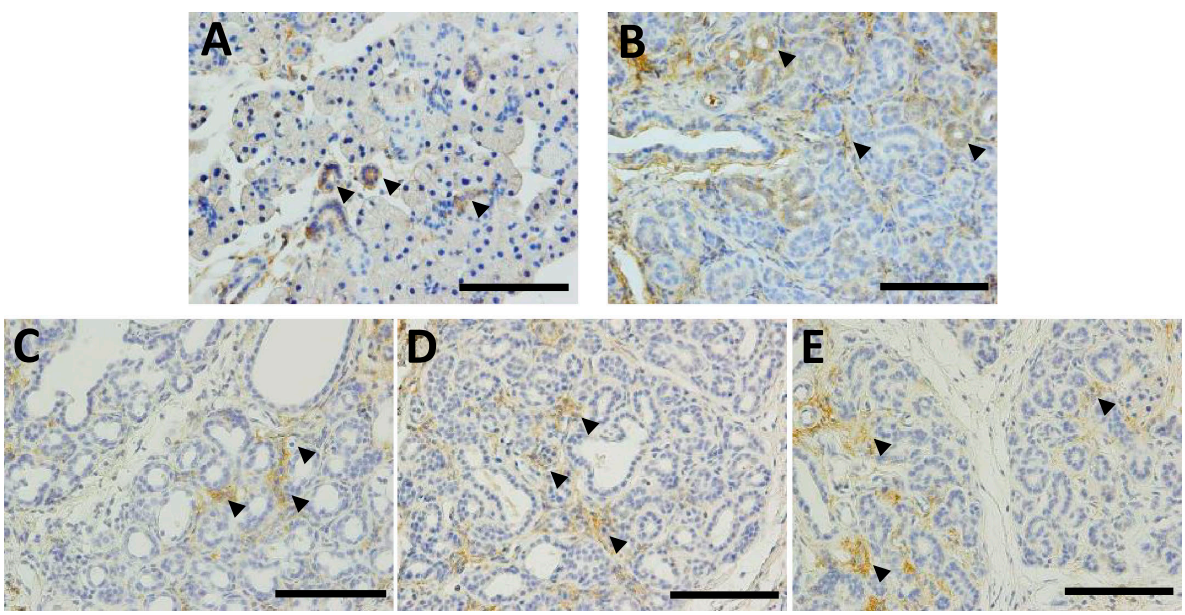

Fig. 2. Immunostaining for the stem cell marker c-kit of the submandibular gland: **A**) controls; **B**) 2-month ligation (2M lig) group; **C**) 2-month ligation, 1 week after release (2M+1W del) group; **D**) 2-month ligation, 1 month after release (2M+1M del) group; **E**) 2-month ligation, 2 months after release (2M+2M del) group. Arrowheads indicate positive staining cells. Bar = 100 μm.

as the formation of salivary calculi. It is believed that long-term duct obstruction leads to irreversible atrophy of the salivary glands, which can become foci of infection, and there is little or no scope for recovery in function. Consequently, the salivary glands are commonly removed in such situations. The recent development of ultra-thin endoscopy has, however, made it possible to crush and remove intraductal salivary calculi, bringing about changes in conventional treatment plans [33]. The structure of the mouse salivary gland differs from that of humans, as the mouse gland contains granular ducts [13]. According to previous studies, granular ducts in male mice after sexual maturity

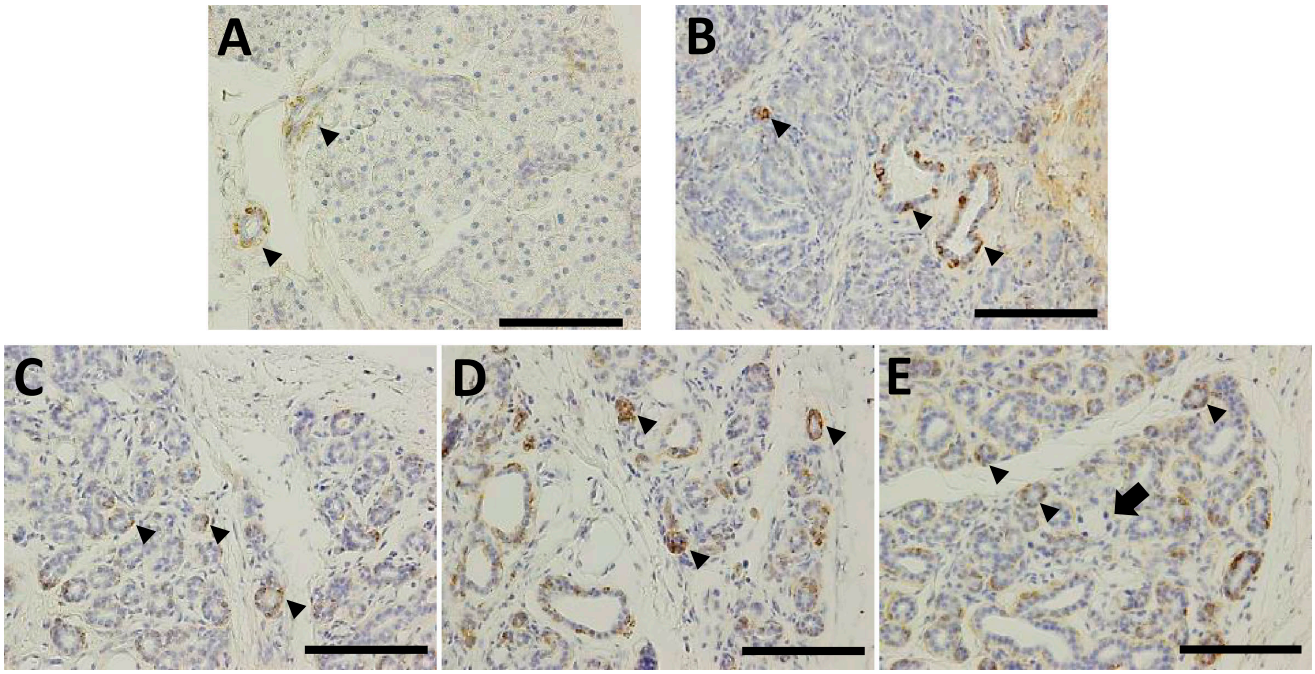

Fig. 3. Immunostaining for the acinar cell precursor marker cytokeratin 5 (CK5) of the submandibular gland: **A**) controls; **B**) 2-month ligation (2M lig) group; **C**) 2-month ligation, 1 week after release (2M+1W del) group; **D**) 2-month ligation, 1 month after release (2M+1M del) group; **E**) 2-month ligation, 2 months after release (2M+2M del) group. Structures are identified as follows: arrow, regenerated acinar portion; arrowheads indicate positive staining cells. Bar = 100 μm.

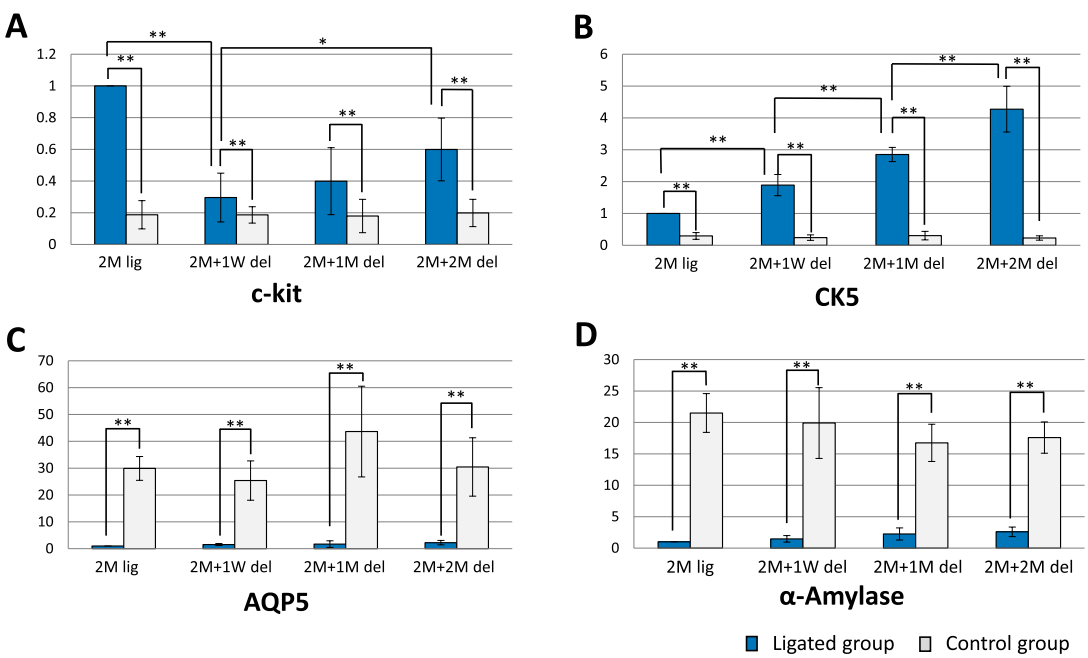

Fig. 4. Real-time reverse transcription polymerase reaction findings in submandibular glands of the 2-month ligation (2M lig) group, the 2-month ligation, 1 week after release (2M+1W del) group, the 2-month ligation, 1 month after release (2M+1M del) group and the 2-month ligation, 2 months after release (2M+2M del) group for: **A**) c-kit; **B**) cytokeratin 5 (CK5); **C**) aquaporin 5 (AQP5) and **D**) α-amylase. Error bars show the standard deviation, n = 5 per group. ** $p < 0.01$, * $p < 0.05$; other differences not significant.

were found to develop at a markedly faster rate than in female mice; moreover, the α-amylase activity in the granular ducts was found to be higher than that in the intercalated and striated ducts. Therefore, considering the role of granular ducts, we elected to use female mice exclusively for this study.

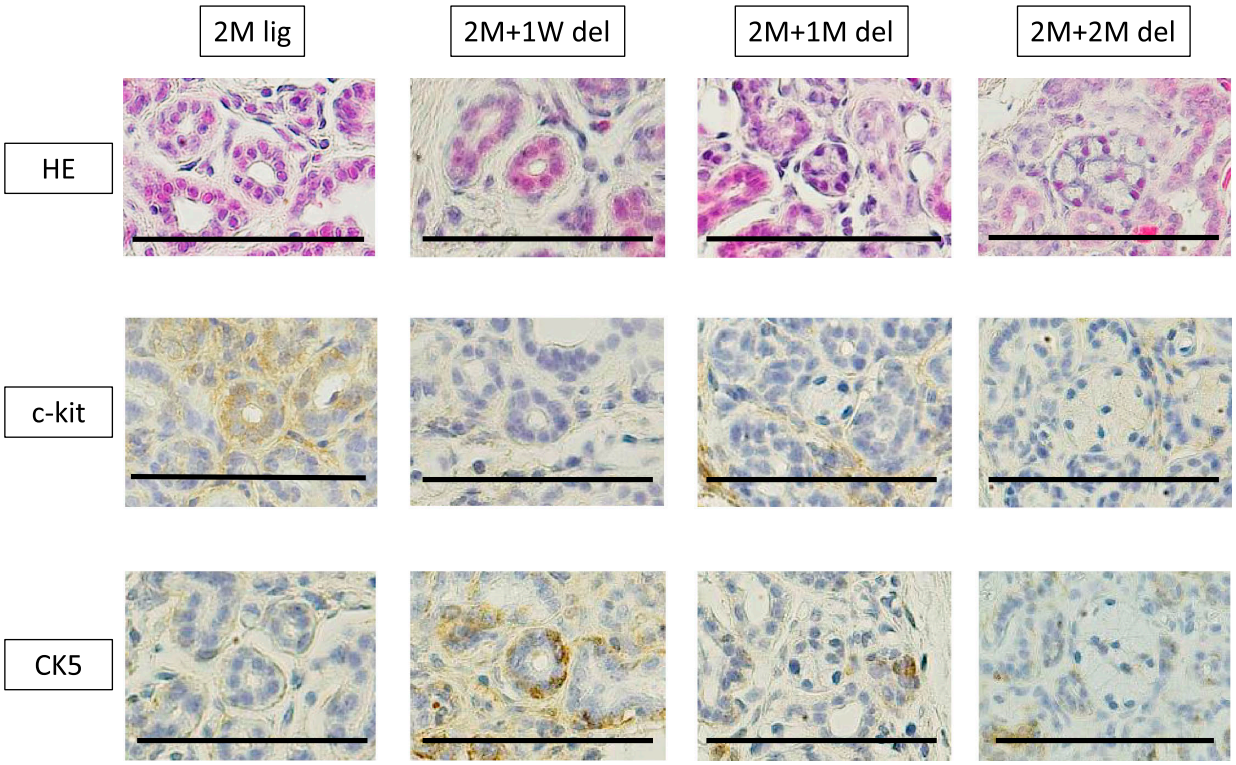

Fig. 5. Magnified views of submandibular tissue stained with hematoxylin-eosin (HE), or for c-kit or cytokeratin 5 (CK5) expression at each time point. Abbreviations: 2M lig, 2-month ligation group; 2M+1W del, 2-month ligation, 1 week after release group; 2M+1M del, 2-month ligation, 1 month after release group; 2M+2M del, 2-month ligation, 2 months after release group. Bar = 100 μm.

If salivary gland tissue can be preserved, functional improvements in atrophied salivary glands may be possible, and the quality of life of patients with obstructive salivary gland disease would be improved. Previous studies of the obstruction and release of obstruction of salivary glands have been conducted over approximately 1 week [23, 27, 28]. We chose to examine changes in glandular tissue structure, residual function and regenerative capacity after the release of submandibular gland obstruction in conditions that more closely mimic those encountered in clinical practice.

We found that long-term ligation of the submandibular duct caused significant shrinkage of the glandular parenchyma, and the dimensions of the gland did not recover after release of ligation. Histologic findings showed submandibular gland atrophy, disappearance of the acinar portion and an increase in duct-like structures and fibrous connective tissue after 2 months of ligation. These findings were similar to those of short-term ligation studies [1, 2, 31, 32, 35]. Gene expression analysis showed low levels of the acinar cell marker AQP5 [11, 13, 16, 25] and the functional marker α-amylase [11, 36], which is consistent with previous results [17]. While obstruction causes histologic atrophy and changes the morphology of the acinar portion, low levels of marker proteins were nonetheless maintained inside the cells. Although the expression of AQP5 and α-amylase did not change after release of ligation, the acinar portion reappeared histologically after 1–2 months. This indicates that even when the acinar portion has atrophied or disappeared after long-term obstruction, regeneration may be possible when the obstruction is removed. Immunohistochemical staining detected the expression of AQP5 in the membrane of acinar cells following the release of ligation, which was thought to regenerate salivary permeability of the acinar cells. Furthermore, periodic acid–Schiff staining also showed positive results in the cytoplasm of the acinar cells, which we judged to represent the production of saliva containing mucin (data not shown). However, neither immunohistochemical staining nor quantitative genetic analysis yielded positive results for α-amylase. Our findings nonetheless revealed that the salivary glands contained components that could regenerate.

Salivary glands develop by branching morphogenesis, like many mammalian excretory organs such as the breast, lung, kidney and prostate [10, 12]. In branching morphogenesis it is reported that the mesenchyme drives differentiation of the epithelium [6, 21]. In this process, c-kit may participate in the proliferation and differentiation of the acinar portion, processes that are important contributors to branching morphogenesis [34]. c-kit has also been reported to play a similar role in stem cells [9, 15]. Expression of c-kit has been reported in some ducts in mature, healthy salivary glands [20, 24, 30], and in and around atrophied salivary glands and duct-like structures [9, 17]. While duct-like structures were initially thought to reflect only regres-

sive changes in the acinar portion, they have since been reported to play a role in their regeneration [18, 22]. When rat submandibular glands were exposed to a laser, duct-like structures were observed to proliferate and to differentiate into an immature acinar portion during regeneration [26]. Cells with high-electron density secretory granules have been reported to differentiate from duct-like structures and to produce a mature acinar portion [31, 32]. Moreover, the differentiation of the acinar portion from duct-like structures reportedly resembles the early stages of the differentiation of the acinar portion from the terminal portion [35]. The terminal portion, along with connective tissue, makes up most of the salivary gland immediately after birth. During the subsequent development of salivary gland tissue, terminal tubule cells become active and proliferate from birth to the age of 2 weeks. By the age of 3 weeks, the acinar portion makes up most of the mature salivary gland tissue, and the terminal portion has mostly disappeared [5, 8, 29]. Therefore, terminal tubule cells are considered to differentiate into acinar cells (i.e., show precursor cell-like characteristics) [37].

This suggests that duct-like structures, which resemble the terminal portion and show the characteristics of acinar precursor cells, play an important role in salivary gland tissue, particularly in regeneration of the acinar portion. From previous studies we know that c-kit expressing cells can contribute to gland regeneration.

The function of CK5 in precursor cells is not well established. It is an epithelial basal cell protein with a molecular weight of 58 kDa. It is recognized as an exocrine gland stem cell marker in the mammary gland, and it has recently been used as a precursor-cell marker [3, 17]. While we found that c-kit expression was elevated after 2 months of ligation, it decreased significantly 1 week after clip removal before rising significantly over the next 2 months. This observation can likely be explained by the homeostatic function of c-kit: its activation stimulates mitosis and prevents apoptosis, and its inhibition induces the process of cell death [14, 34]. In contrast, CK5 expression was significantly lower after ligation and increased after release. Both c-kit- and CK5-positive cells were observed in duct-like structures, suggesting that even atrophied salivary glands retain some regenerative capacity after the release of long-term obstruction, and that duct-like structures are involved in tissue regeneration. Further, CK5 expression was not observed in the acinar portion after clip removal, suggesting that CK5 may be a marker of acinar precursor cells (Fig. 5).

We have not conducted a detailed investigation of cellular dynamics in this study; the examination of the regenerative process from duct-like structures to an acinar portion is a topic for future research. It has recently been reported that Wnt/β-cateni signal transduction is involved in the generation and regeneration of endoderm-derived organs, a pathway that is activated in the short-term obstruction of the main salivary duct in mice, and which is associated with an increase in stem cell and precursor cell populations [7]. Cellular signaling pathways will also need to be examined to illuminate the mechanisms underpinning regeneration after the release of long-term obstruction of the main submandibular duct.

In conclusion, we examined the changes in submandibular gland tissue after release of long-term ligation of the main submandibular excretory ducts in mice, including histologic and gene expression analyses. After the release of ligation, we confirmed the presence of an acinar portion in atrophied submandibular gland tissue, which suggests that it retains some auto-regenerative capacity even after long-term obstruction. Our findings also suggest that CK5 could serve as a marker of the regenerative process.

V. Acknowledgments

We would like to thank Professor Yukio Miyagawa, who assisted with our statistical analysis, and Dr. Masato Mikami for his invaluable advice and support.

VI. References

1. Akadomari, K., Tanaka, A. and Mataga, I. (2016) Regenerative capacity of atrophic submandibular gland by duct ligation in mice. *J. Hard Tissue Biol.* 25; 121–130.
2. Bozorgi, S. S., Proctor, G. B. and Carpenter, G. H. (2014) Rapamycin delays salivary gland atrophy following ductal ligation. *Cell Death Dis.* 27; e1146.
3. Böcker, W., Bürger, H., Buchwalow, I. B. and Decker, T. (2005) Ck5-positive cells are precursor cells of glandular and myoepithelial cell lineages in the human breast epithelium. A new concept as a basis for a better understanding of proliferative breast disease? *Verh. Dtsch. Ges. Pathol.* 89; 45–47.
4. Cotroneo, E., Proctor, G. B., Paterson, K. L. and Carpenter, G. H. (2008) Early markers of regeneration following ductal ligation in rat submandibular gland. *Cell Tissue Res.* 332; 227–235.
5. Cotroneo, E., Proctor, G. B., Paterson, K. L. and Carpenter, G. H. (2010) Regeneration of acinar cells following ligation of rat submandibular gland retraces the embryonic-perinatal pathway of cytodifferentiation. *Differentiation* 79; 120–130.
6. Haara, O., Koivisto, T. and Miettinen, P. J. (2009) EGF-receptor regulates salivary gland branching morphogenesis by supporting proliferation and maturation of epithelial cells and survival of mesenchymal cells. *Differentiation* 77; 298–306.
7. Hai, B., Yang, Z., Millar, S. E., Choi, Y. S., Taketo, M. M., Nagy, A. and Liu, F. (2010) Wnt/β-catenin signaling regulates postnatal development and regeneration of the salivary gland. *Stem Cells Dev.* 19; 1793–1801.
8. Hipkaeo, W., Chomphoo, S., Pakkarato, S., Sakaew, W., Sawatpanich, T., Hozumi, Y., Polsan, Y., Hipkaeo, D., Goto, K. and Kondo, H. (2015) Selective localization of diacylglycerol kinase (DGK)ζ in the terminal tubule cells in the submandibular glands of early postnatal mice. *Histochem. Cell Biol.* 144; 185–193.
9. Hisatomi, Y., Okumura, K., Nakamura, K., Matsumoto, S., Satoh, A., Nagano, K., Yamamoto, T. and Endo, F. (2004) Flow cytometric isolation of endodermal progenitors from mouse salivary gland differentiate into hepatic and pancreatic lineages. *Hepatology* 39; 667–675.
10. Jaskoll, T. and Melnick, M. (1999) Submandibular gland morphogenesis: stage-specific expression of TGF-alpha/EGF,

IGF, TGF-beta, TNF, and IL-6 signal transduction in normal embryonic mice and the phenotypic effects of TGF-beta2, TGF-beta3, and EGF-r null mutations. *Anat. Rec.* 256; 252–268.
11. Kawakami, M., Ishikawa, H., Tanaka, A. and Mataga, I. (2016) Induction and differentiation of adipose-derived stem cells from human buccal fat pads into salivary gland cells. *Hum. Cell* 29; 101–110.
12. Kim, H. Y. and Nelson, C. M. (2012) Extracellular matrix and cytoskeletal dynamics during branching morphogenesis. *Organogenesis* 8; 56–64.
13. Larsen, H. S., Aure, M. H., Peters, S. B., Larsen, M., Messelt, E. B. and Galtung, H. K. (2011) Localization of AQP5 during development of the mouse submandibular salivary gland. *J. Mol. Histol.* 42; 71–81.
14. Lennartsson, J. and Ronnstrand, L. (2012) Stem cell factor receptor/c-Kit: from basic science to clinical implications. *Physiol. Rev.* 92; 1619–1649.
15. Lombaert, I. M., Brunsting, J. F., Wierenga, P. K., Faber, H., Stokman, M. A., Kok, T., Visser, W. H., Kampinga, H. H., de Haan, G. and Coppes, R. P. (2008) Rescue of salivary gland function after stem cell transplantation in irradiated glands. *PLoS One* 3; e2063.
16. Matsuzaki, T., Susa, T., Shimizu, K., Sawai, N., Suzuki, T., Aoki, T., Yokoo, S. and Takata, K. (2012) Function of the membrane water channel aquaporin-5 in the salivary gland. *Acta Histochem. Cytochem.* 45; 251–259.
17. Murayama, K., Kawakami, M. and Tanaka, A. (2017) Chronic changes in the atrophied submandibular gland after long-term ligation of the main excretory duct in mice. *J. Hard Tissue Biol.* 26; 13–22.
18. Nagai, K., Arai, H., Okudera, M., Yamamura, T., Oki, H. and Komiyama, K. (2014) Epiregulin is critical for the acinar cell regeneration of the submandibular gland in a mouse duct ligation model. *J. Oral Pathol. Med.* 43; 378–387.
19. Nanduri, L. S., Maimets, M., Pringle, S. A., van der Zwaag, M., van Os, R. P. and Coppes, R. P. (2011) Regeneration of irradiated salivary glands with stem cell marker expressing cells. *Radiother. Oncol.* 99; 367–372.
20. Nanduri, L. S., Lombaert, I. M., van der Zwaag, M., Faber, H., Brunsting, J. F., van Os, R. P. and Coppes, R. P. (2013) Salisphere derived c-Kit^{+} cell transplantation restores tissue homeostasis in irradiated salivary gland. *Radiother. Oncol.* 108; 458–463.
21. Rebustini, I. T., Hayashi, T., Reynolds, A. D., Dillard, M. L., Carpenter, E. M. and Hoffman, M. P. (2012) miR-200c regulates FGFR-dependent epithelial proliferation via Vldlr during submandibular gland branching morphogenesis. *Development* 139; 191–202.
22. Scott, J., Liu, P. and Smith, P. M. (1999) Morphological and functional characteristics of acinar atrophy and recovery in the duct-ligated parotid gland of the rat. *J. Dent. Res.* 78; 1711–1719.
23. Shimizu, O., Yasumitsu, T., Shiratsuchi, H., Oka, S., Watanabe, T., Saito, T. and Yonehara, Y. (2015) Immunolocalization of FGF-2, -7, -8, -10 and FGFR-1-4 during regeneration of the rat submandibular gland. *J. Mol. Histol.* 46; 421–429.
24. Sumita, Y., Liu, Y., Khalili, S., Maria, O. M., Xia, D., Key, S., Cotrim, A. P., Mezey, E. and Tran, S. D. (2011) Bone marrow-derived cells rescue salivary gland function in mice with head and neck irradiation. *Int. J. Biochem. Cell Biol.* 43; 80–87.
25. Susa, T., Sawai, N., Aoki, T., Iizuka-Kogo, A., Kogo, H., Negishi, A., Yokoo, S., Takata, K. and Matsuzaki, T. (2013) Effects of repeated administration of pilocarpine and isoproterenol on aquaporin-5 expression in rat salivary glands. *Acta Histochem. Cytochem.* 46; 187–197.
26. Takahashi, S. and Wakita, M. (1993) Regeneration of the intralobular duct and acinus in rat submandibular glands after YAG laser irradiation. *Arch. Histol. Cytol.* 56; 199–206.
27. Takahashi, S., Schoch, E. and Walker, N. I. (1998) Origin of acinar cell regeneration after atrophy of the rat parotid induced by duct obstruction. *Int. J. Exp. Pathol.* 79; 293–301.
28. Takahashi, S., Shinzato, K., Nakamura, S., Domon, T., Yamamoto, T. and Wakita, M. (2004) Cell death and cell proliferation in the regeneration of atrophied rat submandibular glands after duct ligation. *J. Oral Pathol. Med.* 33; 23–29.
29. Takahashi-Horiuchi, Y., Sugiyama, K., Sakashita, H. and Amano, O. (2008) Expression of heat shock protein 27 with the transition from proliferation to differentiation of acinar precursor cell in regenerating submandibular gland of rats. *Tohoku J. Exp. Med.* 214; 221–230.
30. Takeyama, A., Yoshikawa, Y., Ikeo, T., Morita, S. and Hieda, Y. (2015) Expression patterns of CD66a and CD117 in the mouse submandibular gland. *Acta Histochem.* 117; 76–82.
31. Tamarin, A. (1971) Submaxillary gland recovery from obstruction. I. Overall changes and electron microscopic alterations of granular duct cells. *J. Ultrastruct. Res.* 34; 276–287.
32. Tamarin, A. (1971) Submaxillary gland recovery from obstruction. II. Electron microscopic alterations of acinar cells. *J. Ultrastruct. Res.* 34; 288–302.
33. Ueda, J., Iwai, T., Ozawa, T., Oguri, S., Mitsudo, K. and Tohnai, I. (2016) Endoscopic removal of submandibular gland stone in a child: a case report. *Jpn. J. Oral Maxillofac. Surg.* 62; 575–578.
34. Wang, X., Qi, S., Wang, J., Xia, D., Qin, L., Zheng, Z., Wang, L., Zhang, C., Jin, L., Ding, G., Wang, S. and Fan, Z. (2014) Spatial and temporal expression of c-Kit in the development of the murine submandibular gland. *J. Mol. Histol.* 45; 381–389.
35. Yagishita, H., Uchida, M. and Aiyama, S. (2001) Histological changes in the rat submandibular gland following ligation and removal of the main excretory duct. *Jpn. J. Oral Biol.* 43; 676–689.
36. Yamagishi, R., Wakayama, T., Nakata, H., Adthapanyawanich, K., Kumchantuek, T., Yamamoto, M. and Iseki, S. (2014) Expression and localization of α-amylase in the submandibular and sublingual glands of mice. *Acta Histochem. Cytochem.* 47; 95–102.
37. Yamamoto, M., Nakata, H., Kumchantuek, T., Sakulsak, N. and Iseki, S. (2016) Immunohistochemical localization of keratin 5 in the submandibular gland in adult and postnatal developing mice. *Histochem. Cell Biol.* 145; 327–339.